

# A Power Market Model with Hyperscalers and Modular Datacenters

Yihsu Chen, *Senior Member, IEEE*, Abel Souza, Fargol Nematkhah, and Andrew L. Liu

**Abstract**—The rapid adoption of AI has led the growth of computational demand, with large language models (LLMs) at the forefront since ChatGPT’s debut in 2022. Meanwhile, large amounts of renewable energy have been deployed but, ultimately, curtailed due to transmission congestion and inadequate demand. This work develops a power market model that allows hyperscalers to spatially migrate LLM inference workloads to geodistributed modular datacenters (MDCs), which are co-located with near renewable sources of energy at the edge of the network. We introduce the optimization problems faced by the hyperscaler and MDCs in addition to consumers, producers, and the electric grid operator, where the hyperscaler enters an agreement to lease MDCs while ensuring that the required service level objectives (SLOs) are met. The overall market model is formulated as a complementarity problem where the proof is provided showing the existence and uniqueness of the solutions. When applying the model to an IEEE RTS-24 bus case study, we show that even with a provision that requires MDCs to disclose the CO<sub>2</sub> emissions associated with their energy supply sources, renting less polluting MDCs is unlikely to yield meaningful emission reductions due to so-called *contract-reshuffling*. The situation can be mitigated when conventional loads are supplied by forward contracts through power purchase agreements. This also leads to a decline in system congestion when the hyperscaler becomes increasingly cost-aware.

**Index Terms**—Datacenters, Hyperscalers, Modular Datacenter, Sustainability, Complementarity Problem.

## I. INTRODUCTION

THE accelerating adoption of artificial intelligence (AI), led by large language models (LLMs) since the launch of ChatGPT in 2022, has marked the beginning of an era defined by massive and rapidly growing datacenter’s computational demand. However, this rapid expansion comes at the expense of unprecedented increases in energy loads. While training LLMs has been widely known as energy-demanding, the energy during the inference phase is often overlooked despite processing millions of real-time queries daily. Many U.S. technology firms are securing dedicated energy sources to support the rapid growth of LLM workloads. Notably, Microsoft has partnered with Constellation Energy to restart the Three Mile Island nuclear plant by 2028 [1], while Google is collaborating with Kairos Power to deploy 500 MW of small

modular reactors between 2030 and 2035 [2]. However, these long development timelines create a near-term bottleneck, constraining the sustainability and scalability of datacenter operations that remain dependent on fossil-fuel-dominated grids.

Data centers are generally categorized into two primary types: hyperscalers and modular data centers (MDCs). Hyperscalers are highly optimized facilities characterized by large-scale, uniform computing architectures; they typically house hundreds of thousands of servers and GPUs [1]. The latter is also known as Edge data centers, i.e., factory built, pre-engineered, and fully tested modular units, having been mostly used by telecommunication companies and mobile operators. It is delivered on a skid or within a container enclosure instead of traditional on-site construction, and has high bandwidth and low latency network capabilities. Because it is pre-built with standardized and repeatable components, it offers scalable capacity and rapid deployment.

Issues related to the sustainable operation of hyperscale datacenters have received increasing attention [3]–[11]. For example, [3] proposed a workload-scheduling algorithm for datacenters with on-site renewables that jointly handles latency-sensitive and delay-tolerant workloads while minimizing processing cost based on electricity prices in the market. Similarly, [4] developed a cloud-computing approach that reduces GHG emissions by routing workloads across distributed datacenters based on marginal rather than average grid emissions, demonstrating the benefit of optimizing workloads based on the marginal emission rate. More recently, [5] presented Ecomap, a sustainability-driven edge computing framework that dynamically adapts power limits and substitutes with less computing demanding models based on real-time carbon intensity. It demonstrated a 30% reduction in emissions while maintaining latency and efficiency. Similarly, [10] proposed an energy-management framework, DynamoLLM, that leverages the unique characteristics of LLM inference workloads (e.g., input and output token counts) to reduce energy consumption by dynamically adjusting GPU frequencies while still meeting performance SLOs (Service Level Objectives).

A common feature of this line of work is that electricity prices and carbon emission rates are treated as exogenous and fixed parameters. In reality, however, large datacenters can materially influence both market prices and marginal emissions [9]. That is, both power prices and marginal emission rates are endogenously determined by market supply and demand, affected by datacenter computing loads. Moreover, marginal emission rates only reflect infinitesimal changes at the operating margin and, therefore, become inappropriate

Y. Chen is with the Environmental Studies Department, the Electrical and Computer Engineering Department, at University of California, Santa Cruz, CA, USA (email: yihsuchen@ucsc.edu).

A. Souza is with the Computer Science and Engineering Department at University of California, Santa Cruz, CA, USA (email: absouza@ucsc.edu).

F. Nematkhah is with the Electrical and Computer Engineering Department at the University of California, Santa Cruz, CA, USA (email: fnematkh@ucsc.edu).

A. Liu is with Edwardson School of Industrial Engineering at Purdue University, West Lafayette, IN, USA (email: andrewliu@purdue.edu).

when evaluating load shifts of non-trivial scale. Consequently, cost savings and emission reductions derived from marginal-emission-based models may not hold when datacenter loads are significant. One exception is [12], which minimizes CO<sub>2</sub> emissions by subjecting the datacenter operation problem to the optimal conditions of the ISO's DC-OPF (Direct-Current Optimal Power Flow) problem. However, this implies that the hyperscaler fully anticipates the decisions by the ISO and generators when making their operation decisions, seemingly deviating from market reality.

Furthermore, an emerging but relatively underexplored strategy is to lease distributed MDCs for computing. When strategically co-located at the edge of the grid, where renewable generation such as wind or solar is frequently curtailed [13], MDCs can absorb otherwise wasted energy, thereby reducing carbon emissions, alleviating grid congestion, and providing flexible computing capacity that complements hyperscalers [14], [15]. Interest in MDC capacity leasing has grown rapidly [6], [16]–[18], with infrastructure providers such as EdgeConneX, Compass Datacenters, and Schneider Electric offering services that enable hyperscalers to deploy capacity quickly in geographically strategic locations. Under these arrangements, firms such as Meta, Google, Amazon, and Microsoft lease MDC capacity rather than expanding existing facilities, allowing them to accommodate growing inference workloads, reduce latency, improve reliability and geographic redundancy, and take advantage of local energy conditions, particularly in regions with significant renewable curtailment.

Despite these promising developments, the implications of MDC capacity leasing regarding emissions, market interactions, and system level impacts remain insufficiently understood, particularly because the development is new. This paper addresses this issue by developing a market model, formulated as a complementarity problem, that considers the decisions faced by conventional consumers, producers, the grid operator, the hyperscaler, and MDCs. We assume that power transactions among suppliers, conventional consumers, the hyperscaler, and MDCs occur through bilateral contracts, allowing the CO<sub>2</sub> footprint associated with workload processing to be explicitly represented.<sup>1</sup> The hyperscaler allocates workloads between local processing and outsourcing while accounting for both processing costs and the associated CO<sub>2</sub> emissions. MDCs are assumed to be strategically co-located at the edges of the transmission network, allowing them to utilize renewable energy that would otherwise be curtailed in the absence of such facilities. All entities procure electricity through bilateral contracts.

Models built on complementarity formulations have been previously used to investigate interactions among emerging entities, the development of new markets, and the implementation of regulatory or policy interventions in the electric power market [21]. The strength of these models stems from their capacity to explicitly characterize the strategic behavior of multiple agents and to represent their interactions via market-clearing conditions, operational constraints, and equi-

librium formulations. Examples include [22] coupled natural-gas and electricity markets to address strategic interactions span multiple infrastructures, [23] examined the interactions between power markets and cap-and-trade systems, and [20] analyzed the Cournot competition among generators under the bilateral and pool-typed electric power market. Finally, [24] showed that while coupling energy storage with renewables can effectively reduce congestion and ramping costs, it may unintentionally increase emissions.

Contracts play a pivotal role in power markets, as they enable both suppliers and loads to hedge against price volatility and other operational risks and have been studied extensively. For example, [25] developed an iterative negotiation scheme that enables suppliers and loads to reach forward power purchase agreements while accounting for price uncertainty and heterogeneous risk preferences. More recently, [26] argued that due to moral hazard and adverse selection issues, the current spot markets alone provide insufficient incentives for zero-carbon investment. A contract of a longer duration can mitigate price volatility and facilitate the funding of the investments. In this paper, we consider a different type of contracts. That is, the capacity leases between the hyperscaler and MDCs, which indirectly affect energy transactions in the electric power market. This paper explicitly analyzes the capacity leasing contracts between the hyperscaler and the MDCs under two emission-disclosure schemes. Under the *ex post* scheme, MDCs report their CO<sub>2</sub> emissions only after operations are completed. In contrast, the *ex ante* scheme requires MDCs to disclose their emission intensities beforehand, enabling the hyperscaler to incorporate these values into its workload allocation decisions.

We have the following central findings. First, both *ex post* and *ex ante* schemes are unlikely lead to meaningful CO<sub>2</sub> benefits due to contract rearrangements among conventional loads, the hyperscalers and MDCs, i.e., contract reshuffling. When conventional loads are served through forward contracts between utilities and suppliers, the extent of contract reshuffling is mitigated, which in turn leads to a reduction in emissions. Second, under the *ex ante* scheme, the prices of capacity-leasing contracts can differ across MDCs when the hyperscaler takes CO<sub>2</sub> emissions into account. In contrast, when processing cost is the sole consideration, all MDCs receive the same leasing price despite differences in their emission intensities and in the types of batches they are capable of processing. This highlights the complexity that emerges from the interaction among the hyperscaler's objectives, the information-disclosure schemes, and the existence of forward contracts in a competitive power market.

The remainder of the paper is organized as follows. Section II describes the optimization problems faced by each entity in the market. Theoretical properties of the models are analyzed in Section III. The models developed in Section II are then applied to a case study of IEEE 24-bus Test System in Section VI. Numerical simulations are conducted to illustrate our findings. Concluding remarks are summarized in Section V.

<sup>1</sup>In fact, bilateral contracts have also been applied to study California's cap-and-trade program [19], and its equivalence to a pool-based market under perfect competition has been formally established in [20].

## II. MODEL

This section presents the optimization problem faced by each entity. The network consists of node  $i \in I$ . The nodes hosting conventional loads, the hyperscalers, and the MDCs are, respectively denoted by  $I^d$ ,  $I^r$ , and  $I^x$ , where the three sets are mutually exclusive. That is,  $I^d \cap I^r = I^d \cap I^x = I^r \cap I^x = \emptyset$ .

### A. Conventional Consumer's Problem

The consumers' willingness to pay in node  $i$  at period  $t$  is represented by an affine benefit function  $B_{it}$ . The utility in node  $i$  procures electricity on behalf of its customers in node  $i$  by entering a power purchase agreement (PPA) with producers. Its objective is given in (1) where  $d_{jhit}$  denotes the energy sales from the power plant  $h$  located in  $j$  to  $i$ , and where the first and second terms represent the total benefit and the payments, respectively.

$$\max_{d_{jhit} \geq 0} \sum_t B_i \left( \sum_{j,h \in H_j} d_{jhit} \right) - \sum_{j,h \in H_j,t} \theta_{jhit}^d d_{jhit} \quad (1)$$

### B. Producer's Problem

Producers solve the profit maximization problem defined in (2) subject to (3), which determines the quantity sold to the utility at node  $i$ , denoted by  $g_{jhit}$ , subject to the capacity constraint in (3). Variables  $\theta_{jhit}^d$ ,  $\theta_{jhit}^x$  and  $\theta_{jhit}^r$  denote the bilateral prices with utilities, the hyperscalers and MDCs, respectively. Note that their values are exogenous to the producers' problem but endogenous to the overall market equilibrium model. The profits include the first three summations in (2) jointly determine the profit, which equals revenue, minus production cost  $C_{jh}$  and the wheeling charge,  $\omega_{jt}$ .<sup>2</sup>

$$\begin{aligned} \max_{g_{jhit} \geq 0} & \sum_{i \in I^x,t} g_{jhit} \theta_{jhit}^x + \sum_{i \in I^r,t} g_{jhit} \theta_{jhit}^r + \sum_{i \in I^d,t} g_{jhit} \theta_{jhit}^d \\ & - \sum_{j,h \in H_j,t} C_{jh} \left( \sum_i g_{jhit} \right) - \sum_{i,j,t} (\omega_{it} - \omega_{jt}) g_{jhit} \end{aligned} \quad (2)$$

$$\text{s.t.} \quad \sum_i g_{jhit} \leq G_{jh} \quad (\lambda_{jht}) \quad (3)$$

### C. The Grid Operator

The grid operator aims to maximize the value of the transmission network by determining the net injection/withdrawal  $y_{it}$  where  $\omega_{it}$  gives the wheeling charge to bring power from the hub to node  $i$  at time  $t$ . The grid operator is subject to the energy balance conditions in (5) and to the lower and upper transmission flow limits in (6) and (7), respectively, where PTDF refers to the Power Transfer Distribution Factors derived from the linearized DC power flow model [27]. A similar formulation has been used else-where, e.g., Metzler et al. [28].

$$\max_{y_{it} \text{ free}} \sum_{i,t} \omega_{it} y_{it} \quad (4)$$

$$\text{s.t.} \quad \sum_i y_{it} = 0 \quad (\gamma_t) \quad \forall t \in T \quad (5)$$

<sup>2</sup>For a detailed discussion on wheeling charges, please refer to [20].

$$-F_k - \sum_{i \in I} \text{PTDF}_{ki} y_{it} \leq 0 \quad (\mu_{kt}^1), \quad \forall k \in K, t \in T \quad (6)$$

$$\sum_{i \in I} \text{PTDF}_{ki} y_{it} - F_k \leq 0 \quad (\mu_{kt}^2), \quad \forall k \in K, t \in T. \quad (7)$$

### D. Modular datacenter's Problem

MDCs are assumed to strategically co-locate at the edge of the network where curtailment constantly occurs. The quantities of expected "curtailed" renewables are denoted by  $\sum_{h \in H_i^w} g_{iht}^c$ . A MDC maximizes its profits by deciding on power purchase contracts  $p_{jhit}$ , leasing contracts with hyperscalers  $k_{bit}^r$ , and spillover quantities  $s_{it}$ . Note as alluded to earlier, not every MDC can process all the batches; in fact, each MDC has a different latency threshold, which can be approximated by the distance between the hyperscaler and MDC [29].

The set of batches that can be processed by the MDCs located in node  $i$  is denoted by  $b \in B_i$ , which is determined by the distance between the hyperscaler and the MDCs as well as processing time, which depends on the complexity of the requests characterized by the input and output tokens [30]. The set of variables controlled by the MDCs collectively is denoted as  $\Phi = \{p_{jhit}, k_{bit}^r, s_{it}\}$ .

The maximization problem faced by the MDCs is in (8)–(11). The first term  $\alpha_{bit} k_{bit}^r \nu$  in the objective function Equation (8) describes the revenue from leasing GPUs to the hyperscaler, where  $\alpha_{bit}$  is the revenue from leasing per unit of GPUs,  $k_{bit}^r$  denotes the leasing capacity, and  $\nu$  denotes the power rating per GPU.  $I^x$  represents the set of nodes with MDCs. The second term represents the power purchase costs, where  $p_{jhit}$  and  $\theta_{iht}^x$  denote the quantity and price of the power purchase agreement with suppliers, respectively.

$$\max_{\Phi \geq 0} \sum_{i \in I^x, b, t} \alpha_{bit} k_{bit}^r \nu - \sum_{j,h \in H_j, t} p_{jhit} \theta_{jhit}^x \quad (8)$$

$$\begin{aligned} \text{s.t.} \quad & \sum_b k_{bit}^r - \sum_{j,h \in H_j} p_{jhit} + s_{it} - \sum_{h \in H_i^w} g_{iht}^c = 0 \quad (\eta_{it}) \\ & \forall i \in I^x, t \in T \end{aligned} \quad (9)$$

$$\sum_b k_{bit}^r - \text{Cap}_i \leq 0 \quad (\rho_{it}) \quad \forall i \in I^x, t \in T \quad (10)$$

$$s_{it} - \sum_{h \in H_i} g_{iht}^c \leq 0 \quad (v_{it}) \quad \forall i \in I^x, t \in T \quad (11)$$

The problem is subject to three constraints. Equation (9) imposes energy balance. Equation (10) limits the energy consumed by the migrated batches to be less than or equal to the capacity of the MDCs. Equation (11) requires that the spillover  $s_{it}$  be less than or equal to the amount of curtailed energy. We next turn to the hyperscaler's problem.

### E. Hyperscale datacenter's Problem

The hyperscale datacenter's problem is given in (12)–(13). The hyperscaler receives inference requests, aggregates them into batches  $q_b$  for  $b \in B$ , and decides whether to process them locally using  $\ell_{bjhit}$  or to send them to MDCs using  $k_{bit}^s$ ,

with decision variables collected in  $\Theta := \{\ell_{bjhit}, k_{bit}^s\}$ . The hyperscaler accounts for both processing costs and associated CO<sub>2</sub> emissions, as reflected in the objective (12), where the term weighted by  $\delta$  captures processing costs and the term weighted by  $1 - \delta$  captures CO<sub>2</sub> emissions. Specifically,  $\sum_{b,i \in I^\kappa, t} \alpha_{bit} k_{bit}^s \nu$  and  $\sum_{b,j,h \in H_j, i \in I^\kappa, t} \ell_{bjhit} \theta_{ijht}^\kappa$  represent local processing and external leasing costs, while  $\sum_{j,h \in H_j, i \in I^\kappa, t} p_{jihit} e_{jh}$  and  $\sum_{b,j,h \in H_j, i \in I^\kappa, t} \ell_{bjhit} e_{jh}$  represent local and external CO<sub>2</sub> emissions, respectively. This formulation corresponds to an *ex post* emission disclosure regime for MDCs. The constraint in (13) ensures that all requests are processed.

$$\begin{aligned} \min_{\Theta \geq 0} & \delta \left( \sum_{b,i \in I^\kappa, t} \alpha_{bit} k_{bit}^s \nu + \sum_{b,j,h \in H_j, i \in I^\kappa, t} \ell_{bjhit} \theta_{ijht}^\kappa \right) \\ & + (1 - \delta) \left( \sum_{b,j,h \in H_j, i \in I^\kappa, t} \ell_{bjhit} e_{jh} + \sum_{j,h \in H_j, i' \in I^\kappa, t} p_{jihit} e_{jh} \right) \\ \text{s.t.} & \sum_{i \in I^\kappa} k_{bit}^s + \sum_{j \in I, h \in H_j, i \in I^\kappa, t} \ell_{bjhit} - q_b = 0 \quad (\psi_{bt}) \\ & \forall b \in B, t \in T \end{aligned} \quad (13)$$

#### F. Market Clearing Conditions

The following five sets of market clearing conditions, (14)–(17) are included for all  $j \in I$ ,  $h \in H_j$ , and  $t \in T$ . The first three conditions define the bilateral contract prices between suppliers and (i) consumers, (ii) hyperscalers, and (iii) MDCs. The fourth condition specifies the leasing prices between hyperscalers and MDCs, while the fifth condition determines the wheeling charge.

$$\theta_{jihit}^d \text{ free, } d_{jihit} - g_{jihit} = 0, \quad \forall i \in I^d \quad (14)$$

$$\theta_{jihit}^x \text{ free, } p_{jihit} - g_{jihit} = 0, \quad \forall i \in I^x \quad (15)$$

$$\theta_{jihit}^\kappa \text{ free, } \sum_b \ell_{bjhit} - g_{jihit} = 0, \quad \forall i \in I^\kappa \quad (16)$$

$$\omega_{it} \text{ free, } y_{it} = \sum_{h \in H_i, j \in I} g_{ihjt} - \sum_{j \in I, h \in H_j} g_{jihit}, \quad \forall i \in I \quad (17)$$

$$\alpha_{bit} \text{ free, } k_{bit}^s - k_{bit}^r = 0, \quad \forall b \in B, i \in I^\kappa. \quad (18)$$

#### G. Equilibrium Models

Given the problems faced by all the entities are convex, a necessary and sufficient condition for an optimal solution to satisfy is given by the following first-order or Karush-Kuhn-Tucker (KKT) conditions, one for each variable.

##### Consumers

$$\begin{aligned} 0 \leq d_{jihit} \perp & -B_i' \left( \sum_{j,h \in H_j} d_{jihit} \right) + \theta_{jihit}^d \geq 0, \\ & \forall j \in I, h \in H_j, i \in I^d, t \in T. \end{aligned} \quad (19)$$

##### Producers

$$\begin{aligned} 0 \leq g_{jihit} \perp & - \sum_{m: \{x, \kappa, d\}} \theta_{jihit}^m + (\omega_{it} - \omega_{jt}) + C_{jh}'(g_{jihit}) \\ & + \lambda_{iht} \geq 0, \quad \forall j \in I, h \in H_j, i \in I, t \in T \end{aligned} \quad (20)$$

$$0 \leq \lambda_{jihit} \perp G_{j,h} - \sum_{i \in I} g_{jihit} \geq 0, \quad \forall j \in I, h \in H_j, t \in T. \quad (21)$$

#### The Grid Operator

For  $\forall i \in I, t \in T$ :

$$y_{it} \text{ free, } \omega_{it} + \sum_{k \in K} \text{PTDF}_{ki} (\mu_{kt}^1 - \mu_{kt}^2) + \gamma_t = 0 \quad (22)$$

$$\eta_{it} \text{ free, } \sum_{i \in I} y_{it} = 0 \quad (23)$$

For  $\forall k \in K, t \in T$ :

$$0 \leq \mu_{kt}^1 \perp -F_k - \sum_{i \in I} \text{PTDF}_{ki} y_{it} \leq 0 \quad (24)$$

$$0 \leq \mu_{kt}^2 \perp \sum_{i \in I} \text{PTDF}_{ki} y_{it} - F_k \leq 0 \quad (25)$$

#### Modular datacenter

$$\begin{aligned} 0 \leq p_{jihit} \perp & -\theta_{jihit}^x - \eta_{it} \leq 0, \\ & \forall j \in I, h \in H_j, i \in I, t \in T \end{aligned} \quad (26)$$

$$\begin{aligned} 0 \leq k_{bit}^r \perp & \alpha_{bit} \nu - \eta_{it} - \rho_{it} \leq 0 \\ & \forall b \in B, i \in I, t \in T. \end{aligned} \quad (27)$$

For  $\forall i \in I, t \in T$ :

$$\eta_{it} \text{ free, } \sum_{b \in B} k_{bit}^r - \sum_{j \in I, h \in H_j} p_{jihit} + s_{it} - \sum_{h \in H_i^\omega} g_{iht}^c = 0 \quad (28)$$

$$0 \leq \rho_{it} \perp \sum_{b \in B} k_{bit}^r - \text{Cap}_i \leq 0 \quad (29)$$

$$0 \leq s_{it} \perp -\eta_{it} - v_{it} \leq 0 \quad (30)$$

$$0 \leq v_{it} \perp s_{it} - \sum_{h \in H_i} g_{iht}^c \leq 0 \quad (31)$$

#### Hyperscalers

$$\begin{aligned} 0 \leq \kappa_{bit}^s \perp & -\delta \nu \alpha_{bit} - \psi_{bt} \leq 0, \\ & \forall b \in B, i \in I^\kappa, t \in T \end{aligned} \quad (32)$$

$$\begin{aligned} 0 \leq \ell_{bjhit} \perp & -\delta \theta_{jihit}^\kappa - (1 - \delta) e_{jh} - \psi_{bt} \leq 0 \\ & \forall b \in B, i \in I^\kappa, t \in T \end{aligned} \quad (33)$$

$$\begin{aligned} \psi_{bt} \text{ free, } \sum_{i \in I^\kappa} k_{bit}^s + \sum_{j \in I, h \in H_j, i \in I^\kappa} \ell_{bjhit} - q_b = 0 \\ & \forall b \in B, t \in T \end{aligned} \quad (34)$$

The market equilibrium problem is then defined as the collection of all KKT conditions (19)–(34), together with the market clearing conditions (14)–(18). The resulting problem can then be solved using complementarity problem solvers such as PATH [31], Knitro [32], and Gurobi [33].

#### H. Ex Ante Emission Disclosure

Alternatively, a hyperscaler may require each MDC to disclose its power purchase agreements along with the corresponding emission intensity. The benefit of doing this a hyperscaler can

directly minimize its associated emissions through a capacity leasing agreement. Under this situation, a hyperscaler tends to provide a more competitive leasing offer to those MDCs with a lower emissions intensity, leading to a higher  $\alpha_{bit}$ .

To study this situation, we modify the aforementioned model by adding a new market clearing condition that calculates the MDCs' emission intensity as follows:

$$\epsilon_{it} = \frac{\sum_{j \in I, h \in H_j} p_{jhit} e_{jh}}{\sum_{j \in I, h \in H_j} p_{jhit}}, \quad \forall i \in I^x, t \in T. \quad (35)$$

We then replace the first term within the parenthesis preceded by  $(1-\delta)$  in (12) with  $\sum_{j \in I^x} \epsilon_{it} \kappa_{bit}^s$ . This yields the following condition for  $\kappa_{bit}^s$ .

$$0 \leq \kappa_{bit}^s \quad \perp \quad -\delta \nu \alpha_{bit} - (1-\delta) \epsilon_{it} - \psi_{bt} \leq 0, \quad \forall b \in B, i \in I^x, t \in T \quad (36)$$

Note it is the term  $(1-\delta) \epsilon_{it}$  in (36) that drives a wedge, leading to each MDC subject to a different  $\alpha_{bit}$  compared to (32). We illustrate this observation in the numerical case study in Section IV below.

### III. THEORETICAL ANALYSIS

This section reformulates the equilibrium conditions as a single mixed linear complementarity problem (MLCP), establishes existence, and proves uniqueness of certain aggregate quantities using monotonicity of the associated operator.

#### A. MLCP Formulation

To express the MLCP in a compact matrix form, we require explicit functional forms for the consumer benefit functions  $B_i(\cdot)$  in (1) and the power producer cost functions  $C_{ih}(\cdot)$  in (3). We hence impose the following standing assumption:

*Assumption 1 (Affine marginal benefit and marginal cost):* For each  $i \in I^d$  and  $t \in T$ , the marginal benefit is affine in the total consumption,

$$B'_i \left( \sum_{j \in I, h \in H_j} d_{jhit} \right) = b_{it}^0 - \sum_{j \in I, h \in H_j} b_{it}^1 d_{jhit}, \quad b_{it}^1 \geq 0. \quad (37)$$

For each producer  $(i, h, t)$ , the marginal cost is affine in the bilateral quantity,

$$C'_{jh}(g_{jhit}) = c_{jh}^0 + c_{jh}^1 g_{jhit}, \quad c_{jh}^1 \geq 0. \quad (38)$$

An affine marginal benefit function with  $b_{it}^1 \geq 0$  implies a concave quadratic total benefit function and, equivalently, a downward sloping inverse demand function. Empirical evidence suggests that aggregate electricity demand response to price fluctuations is well-approximated by linear specifications over relevant operating ranges [34].

On the supply side, an affine marginal cost (with  $c_{jh}^1 \geq 0$ ) implies a convex quadratic total cost function. In power system modeling, the heat rate curve of thermal generators, including coal, gas, and oil units, is commonly represented as a quadratic function of output, which directly yields a linear marginal cost. This modeling practice is well documented in classic power system references such as [35].

We next define the decision vectors used in this formulation.

Let the nonnegative variable vector be defined as

$$z := (d, g, \lambda, \mu^1, \mu^2, p, k^r, s, \rho, v, k^s, \ell) \in \mathbb{R}_+^{n_z}, \quad (39)$$

where each block stacks the corresponding components  $\{d_{jhit}\}, \{g_{ihjt}\}, \{\lambda_{iht}\}, \{\mu_{kt}^1\}, \{\mu_{kt}^2\}, \{p_{jhit}\}, \{k_{bit}^r\}, \{s_{it}\}, \{\rho_{it}\}, \{v_{it}\}, \{k_{bit}^s\}$ , and  $\{\ell_{bjhit}\}$ , over all indices defined in Section II.

Similarly, define the vector of free variables as

$$\pi := (\theta^d, \theta^x, \theta^\kappa, \omega, \alpha, y, \gamma, \eta, \psi) \in \mathbb{R}^{n_\pi}, \quad (40)$$

stacking  $\{\theta_{ihjt}^d\}, \{\theta_{ihjt}^x\}, \{\theta_{ihjt}^\kappa\}, \{\omega_{it}\}, \{\alpha_{bit}\}, \{y_{it}\}, \{\gamma_{it}\}, \{\eta_{it}\}$ , and  $\{\psi_{bt}\}$ .

With the above notation and Assumption 1, all KKT conditions (19) – (34) can be stacked into a compact MLCP in matrix form as follows:

$$0 \leq z \quad \perp \quad Mz + N\pi + q \geq 0, \quad (41a)$$

$$N^\top z = r, \quad (41b)$$

where  $M \in \mathbb{R}^{n_z \times n_z}$ ,  $N \in \mathbb{R}^{n_z \times n_\pi}$ ,  $q \in \mathbb{R}^{n_z}$ , and  $r \in \mathbb{R}^{n_\pi}$ . To present the details of the matrices and vectors, we will need additional notations. Define the block diagonal matrix:

$$H_d := \text{diag}(b_{it}^1) \otimes I_{|I| \times |H|}, \quad (42)$$

where each  $(i, t)$  diagonal entry  $b_{it}^1$  is replicated across all  $(j, h)$  components of  $d_{jhit}$ , with  $b_{it}^1$  being the coefficient in the marginal benefit function (37). The sign  $\otimes$  denotes the Kronecker product; that is, for generic matrices  $A \in \mathbb{R}^{m \times n}$  and  $B \in \mathbb{R}^{p \times q}$ ,  $A \otimes B \in \mathbb{R}^{mp \times nq}$  is the block matrix whose  $(i, j)$ th block equals  $A_{ij}B$ . Since  $b_{it}^1 \geq 0$ , it follows directly that  $H_d$  is positive semi-definite (PSD). Similarly, define

$$H_g := \text{diag}(c_{jh}^1), \quad (43)$$

with  $c_{jh}^1$  being the coefficient in the marginal cost function (38).  $H_g$  is also PSD with  $c_{jh}^1 \geq 0$ .

Next, we define a matrix  $A_\lambda \in \mathbb{R}^{|\mathcal{I}_\lambda| \times |\mathcal{I}_g|}$  component-wise as follows. For any row index  $(i, h, t) \in \mathcal{I}_\lambda$  and any column index  $(i', h', j', t') \in \mathcal{I}_g$ ,

$$(A_\lambda)_{(i,h,t),(i',h',j',t')} = \begin{cases} 1, & \text{if } i = i', h = h', t = t', \\ 0, & \text{otherwise,} \end{cases} \quad (44)$$

which is referred to as producer generation incidence matrix such that  $(A_\lambda g)_{iht} = \sum_j g_{ihjt}$ . Then the  $M$  matrix in (41a) can be written as

$$M := \begin{bmatrix} H_d & 0 & 0 \\ 0 & H_g & A_\lambda^\top \\ 0 & -A_\lambda & 0 \end{bmatrix}, \quad (45)$$

where each zero denotes a block of appropriate dimension filled with zeros.

The non-square matrix  $N$  in (41a) and (41b) collects the coefficients of the free variables  $\pi$  in the complementarity conditions. The vector  $q$  collects the constants in the complementarity conditions, while  $r$  collects the constant right-hand sides of the linear equality constraints. Their specific forms are provided in Appendix A.

## B. MLCP Solution Existence

A pair  $(z^*, \pi^*)$  satisfying (41a) and (41b) is called a solution of the MLCP and corresponds to a market equilibrium. We establish existence of such a solution using the matrix properties of (41). To do so, we need another assumption as follows.

*Assumption 2 (Feasibility to meet batch load):* The batch load  $q_b$  for all  $b \in B$  can be supplied by available generators without violating their capacity constraints or transmission limits; that is, for the given generation capacity  $G$  and transmission line capacity  $F$ , the set  $\mathcal{F} := \{(\ell, g, y) \in \mathbb{R}_+^{n_\ell} \times \mathbb{R}_+^{n_g} \times \mathbb{R}^{n_y} \mid (16), (17), (21), (23), (24), (25), (34)\}$  is nonempty.

This assumption can be verified by solving a linear optimization problem: fix  $t \in T$  and define  $Q_t := \sum_{b \in B} q_b$ . Let  $\Lambda_t^*(G, F)$  denote the optimal objective function value of the following linear program, parameterized by  $(G, F)$ :

$$\begin{aligned} & \max_{g \geq 0, y \text{ free}} \sum_{j \in I} \sum_{h \in H_j} \sum_{i \in I^\kappa} g_{jh it} \\ & \text{s.t.} \quad \sum_{i \in I^\kappa} g_{jh it} \leq G_{jh}, \quad \forall j \in I, h \in H_j, \\ & \quad y_{it} = \sum_{h \in H_i, j \in I} g_{ih jt} - \sum_{j \in I, h \in H_j} g_{jh it}, \quad \forall i \in I, \\ & \quad \sum_{i \in I} y_{it} = 0, \\ & \quad -F_k \leq \sum_{i \in I} \text{PTDF}_{ki} y_{it} \leq F_k, \quad \forall k \in K. \end{aligned}$$

It is straightforward to verify that  $\mathcal{F} \neq \emptyset$  if and only if  $Q_t \leq \Lambda_t^*(G, F)$ . A formal proof is omitted due to space limitations.

*Theorem 1 (Existence of equilibrium):* Under Assumption 1 and 2, the MiCP (41) admits at least one solution  $(z^*, \pi^*)$ .

*Proof:* We first establish feasibility of the MLCP; namely, there exist  $(z, \pi)$  with  $z \geq 0$  such that  $Mz + N\pi + q \geq 0$  and  $N^\top z = r$ . Fix a  $t \in T$ , we can construct a feasible point as follows. Choose  $(\ell, g, y) \in \mathcal{F}$ . By definition of  $\mathcal{F}$ , the generation variables satisfy  $g_{jh it} = \sum_b \ell_{bj hit}$  for all  $i \in I^\kappa$ ,  $j \in I$ , and  $h \in H_j$ . For all  $i \in I \setminus I^\kappa$ , set  $g_{jh it} = 0$  for all  $j \in I$  and  $h \in H_j$ . For all  $i \in I$ , define  $s_{it} := \sum_{h \in H_i^\omega} g_{ih t}^c$ . Set the remaining variables  $(d, p, k^r, k^s, \rho, v, \mu^1, \mu^2, \lambda, \omega, \alpha, \psi, \theta^\kappa)$  all equal to zero. Under this construction, the equality constraints (14)–(18), (22), and (28) are satisfied, as are the inequality constraints in (29) and (31)–(33).

For the remaining inequalities, set  $\theta^d = b^0$  with matching dimension, where  $b^0$  is the constant appearing in (37). This guarantees the inequality in (19). Next, choose a scalar  $L > 0$  sufficiently large and define  $\theta^\kappa = -L\mathbf{1}, \eta = L\mathbf{1}$ , where  $\mathbf{1}$  denotes a vector of ones of appropriate dimension. With this choice, the inequalities in (20), (26), (27), and (30) all hold. All remaining constraints follow directly from  $(\ell, g, y) \in \mathcal{F}$ .

Hence, the MLCP (41) is feasible. For the matrix  $M$  defined in (45), since both  $H_d$  and  $H_g$  are PSD, so is  $M$  by definition; that is,  $x^\top Mx \geq 0 \quad \forall x \in \mathbb{R}^{n_z}$ , where  $n_z$  is the dimension of  $M$ . By Lemma EC.1 in [19], an MLCP of the form (41) is solvable (that is, a solution exists) if it is feasible and the matrix  $M$  is PSD. Therefore, the MLCP admits a solution. ■

## C. MLCP Solution Uniqueness

The preceding results establish the existence of a market equilibrium, which may be not unique in general. This raises the question of whether numerical solutions are meaningful for analysis. Following the approach in [19], [36], we can show uniqueness of quantities in the following result.

*Theorem 2 (Uniqueness of weighted demand and generation):* Under Assumptions 1 and 2, for any two equilibria  $(z^1, \pi^1)$  and  $(z^2, \pi^2)$ , we have  $H_d d^1 = H_d d^2$  and  $H_g g^1 = H_g g^2$ , where  $H_d$  and  $H_g$  are defined in (42) and (43). Consequently, the aggregate demand  $D_{it} := \sum_{j \in I} \sum_{h \in H_j} d_{jh it}$  is unique. If, in addition,  $b_{it}^1 > 0$  for all  $i \in I, t \in T$  and  $c_{jh}^1 > 0$  for all  $j \in I, h \in H_j$ , then  $d_{jh it}$  is unique, and the corresponding bilateral generation  $g_{jh it}$  is also unique.

*Proof:* Define  $M_s := \frac{1}{2}(M + M^\top)$ . With  $M$  given in (45), we have  $M_s = \text{diag}(H_d, H_g, 0)$ . As discussed earlier, both  $H_d$  and  $H_g$  are PSD, and hence  $M_s$  is PSD. Lemma EC.2 in [19] implies that for any two solutions of a feasible MLCP of the form (41) with  $M_s$  PSD, one has  $M_s z^1 = M_s z^2$ . Therefore,  $H_d d^1 = H_d d^2$  and  $H_g g^1 = H_g g^2$ . If  $b_{it}^1 > 0$ , then  $H_d$  is positive definite on the subspace indexed by  $(i, t)$ , implying  $d_{jh it}^1 = d_{jh it}^2$  for all  $(j, h)$ . Similarly, if  $c_{jh}^1 > 0$ , then  $(H_g g)^1 = (H_g g)^2$  implies  $g_{jh it}^1 = g_{jh it}^2$ . ■

## IV. NUMERICAL CASE STUDY

### A. Data, Assumptions, and Scenarios

We apply the IEEE Reliability Test System (RTS 24-Bus) [37] to illustrate the model described in Section II. The system consists of 24 buses, 38 transmission lines, and 17 constant-power loads with a total of 2,850 MW. Our analysis groups 32 generators into 13 generators by combining those with the same marginal cost and located at the same node. 6 hydropower units are excluded from the dataset given they are operated at their maximum output of 50MW [38]. We assume that all generators are owned by a single firm, as the analysis does not focus on market power. To generalize the results, the transmission limit of each line is reduced to 60% in order to produce non-uniform LMPs (Locational Marginal Prices). The marginal cost of generation is modeled as a linear function of output, parameterized by the coefficient vectors  $C^0$  and  $C^1$ , whose elements  $c_{jh}^0$  and  $c_{jh}^1$  are defined in (38). We assume a hyperscaler is located at node 24, where three MDCs are situated in nodes 11, 12, and 17. Node 24 is one of the nodes that experiences a lower power price at the baseline.<sup>3</sup>

The RTS 24-Bus case is first solved as a least-cost minimization problem with fixed nodal load to obtain the dual variables. The dual variables, coupled with an assumed price elasticity of -0.2, are then used to define affine inverse demand function. The estimated price elasticity of demand is consistent with findings from previous studies [40].

We examine the ability of a hyperscaler to pursue sustainability (i.e., lowering CO<sub>2</sub> emissions) by leasing computing

<sup>3</sup>In fact, analysis in [39] indicates that energy expenditures account for more than 40% of total datacenter operating costs. Hyperscalers owned by major technology companies often collaborate with utilities to secure discounted long-term tariffs. Recent debates have centered on the extent to which other consumers bear a disproportionate share of the fixed costs induced by the rapid expansion of datacenters and the impact on local communities.

infrastructure from MDCs. These MDCs are strategically co-located at the edge of the network, where renewable energy is frequently curtailed due to insufficient demand or limited transmission capacity.

We assume that MDC1 can process all five batches, MDC2 can process only batches 1–3, and MDC3 can handle only batches 4 and 5. The endowed “curtailed” renewables for three MDCs equal to 2, 4, and 5 MWh, respectively. The workload in MW that needs to be processed by the hyperscaler is equal to 75, 42, 51, 48 and 69, all in MW for types 1–5, respectively. All batches collectively account for roughly 10% of the baseline loads.

Our primary results focus on two scenarios: 1)  $\delta = 0.1$  refers to the case when the hyperscaler is concerned more about CO<sub>2</sub> emissions, and 2)  $\delta = 0.9$  refers to the case when the hyperscaler is concerned more about processing costs. For each case, we investigate two emission disclosure schemes: *ex ante* and *ex post*. We also examine the impact of the hyperscaler’s preference, denoted by  $\delta$ , on CO<sub>2</sub> emissions, processing costs, and leasing costs in Section IV-D.

### B. Ex Post Disclosure

We first discuss the results of “*ex post*” emission disclosure in Table I(a)–III(a) for cost, emissions and emission intensity, respectively, with a focus on two cases with  $\delta = 0.1$  (emissions) and  $\delta = 0.9$  (costs). Note that in both cases, the hyperscaler processes 74% of workload locally.

Table I(a) suggests when the hyperscaler concerns more about emissions ( $\delta = 0.1$ ), the operator is willing to pay more (0.913 vs. 0.156 \$/GPU, reported in Table III(a) bottom panel) to have the workload processed by MDCs since they are powered by curtailed renewables. The total processing cost under  $\delta = 0.9$  is equal to \$71,983, which is significantly lower than that under  $\delta = 0.1$  at \$150,295.

TABLE I: Results: Processing costs [\$] (top) & Average Procurement cost[\$/MWh] (bottom)

(a) Ex Post			(b) Ex Ante		
[\$]	$\delta = 0.1$	$\delta = 0.9$	[\$]	$\delta = 0.1$	$\delta = 0.9$
Local	113,031	65,617	Local	124,367	66,188
MDCs	37,264	6,366	MDCs	3,636	5,701
Total Cost	150,295	71,983	Total Cost	128,023	71,888
MDC1	58.89	58.89	MDC1	61.06	58.57
MDC2	52.91	52.91	MDC2	55.44	52.31
MDC3	0.00	0.00	MDC3	0.00	0.00

Table II(a) summarizes the emissions from three sources: local processing at the hyperscaler, outsourced processing at MDCs, and total system emissions. To our surprise, when the hyperscaler focuses more on cost (i.e.,  $\delta = 0.9$ ), its operation can actually also result in a lower level of emissions from outsourcing workloads to MDCs while emissions with the hyperscaler is almost equal. The workload-related CO<sub>2</sub> footprint under  $\delta = 0.9$  is reduced by 3.56 t (= 39.59–43.15), or approximately 8%. This is because *ex post* scheme is not a good instrument and thus provides an imperfect single to guide the hyperscaler operator to lower emissions as it cannot distinguish MDCs with different emission intensities. Interestingly, overall system emissions do not alter between these two cases, suggesting that the decline in MDCs emissions is offset by an

increase in emissions associated power sales of conventional loads. This observation is dubbed contract reshuffling. We illustrate how this can be mitigated in subsection IV-D.

TABLE II: Results: Emissions [t]

(a) Ex Post			(b) Ex Ante		
	$\delta = 0.1$	$\delta = 0.9$		$\delta = 0.1$	$\delta = 0.9$
Local	32.51	32.51	Local	34.50	32.51
MDCs	10.64	7.08	MDCs	1.40	6.46
Total	43.15	39.59	Total	35.90	38.97
System	1,362.76	1,362.76	System	1,361.50	1,370.41

Table III(a) also reports the emission intensity by MDCs. Except MDC3, which has an intensity of 0 kg/MWh as it is powered only by renewables, the other two MDCs enter power purchase agreements with suppliers. The fact that emissions are disclosed *ex post* means that the hyperscaler does not have information to price GPU leasing differently based on emission intensity and thus leads to the same leasing offer for each MDC.

TABLE III: Results: Emission rate [kg/MWh] (top) & leasing cost [\$/GPU] (bottom)

(a) Ex Post			(b) Ex Ante		
	$\delta = 0.1$	$\delta = 0.9$	[kg/MWh]	$\delta = 0.1$	$\delta = 0.9$
MDC1	621.0	621.0	MDC1	621.1	559.1
MDC2	739.0	145.0	MDC2	621.0	145.0
MDC3	0.0	0.0	MDC3	0.00	0.00
MDC1	0.913	0.156	MDC1	0.036	0.127
MDC2	0.913	0.156	MDC2	0.033	0.152
MDC3	0.913	0.156	MDC3	0.930	0.157

### C. Ex Ante Disclosure

The workload processing costs under the *ex ante* scheme are reported in Table I(b). The hyperscaler maintains total costs at \$71,888 under  $\delta = 0.9$ , comparable to the *ex post* case (\$71,983). In contrast, when  $\delta = 0.1$ , overall workload costs decrease by 34%, from \$150,295 in Table I(a) to \$128,023 in Table I(b). Under *ex ante* disclosure, the hyperscaler observes MDC emission intensities and therefore values MDC capacity leasing less as  $\delta$  increases and as emission intensity rises (see Section IV-D). For example, when emission intensity is 0 t/MWh, Table III(b) shows that the hyperscaler is willing to pay \$0.930/GPU for MDC3 at  $\delta = 0.1$ , compared to \$0.157/GPU at  $\delta = 0.9$ . A similar pattern appears under the *ex post* scheme, although interpretation is complicated because emission profiles are not distinguished. For a given  $\delta$ , lower MDC emission intensity leads to higher capacity leasing prices under *ex ante* disclosure. Consistent with this, MDC1 and MDC2 command higher leasing prices under  $\delta = 0.9$  than under  $\delta = 0.1$ , for example \$0.127 versus \$0.036 for MDC1 and \$0.152 versus \$0.033 for MDC2. This differentiation does not arise under *ex post* disclosure. Despite these pricing effects, overall system emissions in Table II(b) remain comparable to those in Table II(a), indicating that *ex ante* disclosure alone does not yield meaningful sustainability gains.

### D. Sensitivity Analysis

Figure 1 shows the leasing costs of the three MDCs as a function of  $\delta$ . The solid blue denotes the *ex post* scheme while

the color-coded dashed lines represent the *ex ante* scheme for three MDCs. Under the *ex post* scheme, the hyperscaler is only aware of CO<sub>2</sub> after the fact. Thus, its willingness to pay for outsourcing workload is the same for all three MDCs. However, when the hyperscaler becomes aware of the respective emission impact of each MDC under the *ex ante* scheme before the fact, as allude to earlier, the operator's willingness to pay for the services then also depends on the emission intensity of each MDC in Fig. 2. Given MDC3 has no emission, the capacity leasing cost curve of MDC3 lies above the other two MDCs until the  $\delta$  approaches 1 where the processing cost is the only concern.

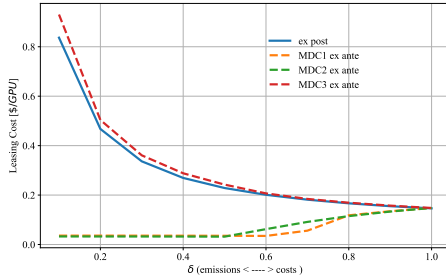


Fig. 1: MDC leasing costs against  $\delta$

However, the comparison between MDC1 and MDC2 is less clear. Because MDC2 is able to procure power at a lower price by an average of 6\$/MWh across the scenarios, the owner is willing to operate the facility at a lower capacity leasing price (for  $\delta$  between 0.5 and 0.7) while still maintaining its profit margin even though its emission intensity is lower as alluded to in Fig. 2. Overall, as  $\delta$  approaches 1, emission intensity is no longer a concern for the hyperscaler, eventually leading to identical leasing prices for all MDCs.

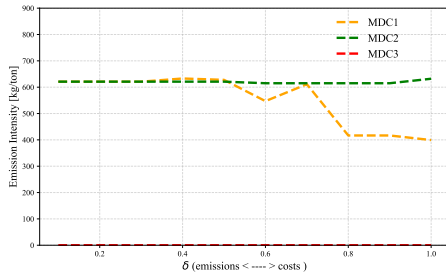


Fig. 2: MDC CO<sub>2</sub> emission rate against  $\delta$

Figures 3–4 present datacenter workload related processing costs and CO<sub>2</sub> emissions for the *ex post* and *ex ante* disclosure cases in panels (a) and (b), respectively. Each figure shows three components: workloads processed locally by the hyperscaler (red dashed line), workloads outsourced to MDCs (green dashed line), and total quantities (blue dashed line). In both disclosure regimes, increasing  $\delta$  shifts the datacenter toward cost minimization, resulting in lower local and total processing costs, as shown in Fig. 4. At the same time, CO<sub>2</sub> emissions rise and eventually spike as  $\delta$  approaches 1, as shown in Fig. 3, when processing cost becomes the dominant objective. Collectively, these figures illustrate a trade off between CO<sub>2</sub>

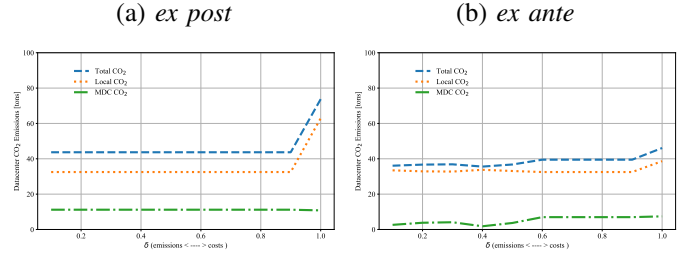


Fig. 3: datacenters workload CO<sub>2</sub> emissions against  $\delta$

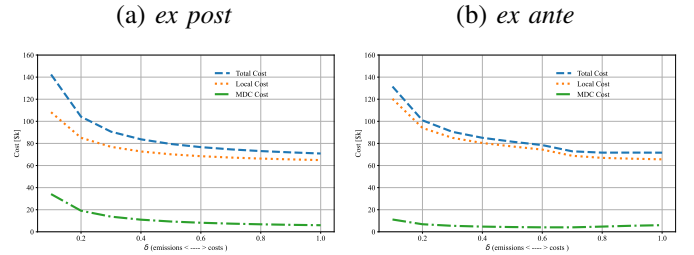


Fig. 4: datacenters workload processing costs against  $\delta$

emissions and total processing costs. Across all cases under both schemes, however, total system CO<sub>2</sub> emissions remain essentially unchanged, indicating that contract re arrangement among conventional consumers, MDCs, and the hyperscaler yields no meaningful emission reduction. We examine the role of forward contracts in the next section.

### E. Forward Contract

In the previous analysis, we assumed that consumers, the hyperscaler, and the MDCs simultaneously entered into power purchase agreements (PPAs) to secure their energy supplies. However, in reality, local utilities, which procure electricity on behalf of consumers, may engage in forward contracts to secure energy supplies and mitigate market risk. These arrangements limit the extent to which datacenters, i.e., hyperscalers and MDCs, can claim renewable energy benefits. To examine this, the analysis sets a lower bound of  $g_{ihjt}$ , ranging from 60%–90%, defined by the baseline at which the processing loads of datacenters equal zero. In other words, this represents the bilateral contract position of conventional loads in the absence of datacenters. The higher the bound is, the more limited that the datacenter can explore contracts to minimize its CO<sub>2</sub> footprint.

Figure 5(a) plots total system CO<sub>2</sub> emissions as a function of  $\delta$  under forward contract requirements ranging from 60% to 90% in the *ex ante* scheme. The solid black line indicates the maximum system-wide emissions of 1,370 t. For contract positions below 90%, emission reductions are achievable for  $\delta \leq 0.6$ , depending on the hyperscaler's concern for CO<sub>2</sub> reductions. The magnitude of this reduction is inversely related to the forward contract position. When the forward contract requirement is set at 90%, leaving only 10% procurement flexibility for datacenters, the system exhibits a modest emission reduction of 2–5% relative to the baseline. This highlights that contract re-shuffling can be mitigated by forward contracts. Figure 5(b) displays the results on network congestion. The

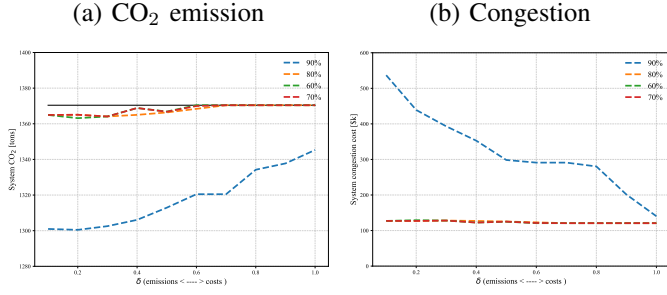


Fig. 5: Total system CO<sub>2</sub> emissions and congestion cost against  $\delta$  under different forward contract positions for the *ex ante* scheme

solutions show that under 60%-80% forward contract cases, there is little impact on the system congestion because of the occurrence of contract re-shuffling. However, under 90% case, as the hyperscaler becomes more cost-aware (toward the right), it allocates more workload to the MDCs in order to lowering processing costs, leading to a decline of the system congestion.

## V. CONCLUSIONS

Since the debut of ChatGPT in 2022, issues related to sustainable operation of datacenters, including hyperscalers and MDCs, have been at the forefront of debates. This paper studies the capacity leasing contract between the hyperscaler and MDCs by developing a power market model, formulated as complementarity problems considering the optimizations faced by conventional consumers, producers, the grid operator, the hyperscaler and MDCs. We consider two emission disclosure schemes. Under the *ex post* scheme, MDCs report their CO<sub>2</sub> emissions after the fact, whereas the *ex ante* scheme enables the hyperscaler to evaluate the emissions implications of its workload allocation decisions based on each MDC's reported carbon intensity in PPAs.

We show that the *ex ante* scheme can, in principle, reduce CO<sub>2</sub> emissions by pricing the capacity leasing contract according to the MDCs' emission intensities. However, this benefit is unlikely to materialize in practice due to contract reallocation among market participants. We further demonstrate that moderate emission reductions are possible in our application to the RTS-24 system when conventional loads are subject to forward contract requirements. This highlights that claims of "100% renewable-powered" datacenters may be misleading unless they correspond to verifiable, short-run emission reductions or are supported by newly developed renewable resources dedicated to the operations of datacenters.

Our analysis is subject to several limitations. First, we assume that all batches yield the same revenue regardless of latency requirements. In practice, some inferences are more time sensitive, such as those requested by users subscribed to higher tier services, and therefore generate higher value. In this case, an MDC capable of processing a wider range of batches could generate greater revenue for the hyperscaler, leading the hyperscaler to offer higher capacity leasing prices and resulting in differential pricing outcomes. Second, we assume that the amount of renewable energy that would otherwise

be curtailed is fixed. In practice, capacity leasing prices may depend on the hyperscaler's expectations of future curtailment levels, which would require a stochastic framework to capture this uncertainty. We leave these extensions to future work.

## APPENDIX A

### THE MLCP FORMULATION – ADDITIONAL DETAILS

The matrix  $N$  in (41) collects the coefficients of the free variables  $\pi$  in the KKT conditions. Consistent with the ordering of the variables in  $z$  and  $\pi$  defined in (39) and (40), the nonzero block rows of  $N\pi$  are  $(N\pi)_d = E_d\theta^d$ ,  $(N\pi)_g = -E_g^d\theta^d - E_g^x\theta^x - E_g^k\theta^k + A_\omega\omega$ ,  $(N\pi)_{\mu^1} = A_{\mu y}y$ ,  $(N\pi)_{\mu^2} = -A_{\mu y}y$ ,  $(N\pi)_p = E_p^x\theta^x + E_{p\eta}\eta$ ,  $(N\pi)_{kr} = E_{kr\eta}\eta - \nu E_{kr\alpha}\alpha$ ,  $(N\pi)_s = E_{s\eta}\eta$ ,  $(N\pi)_{k^s} = \delta\nu E_{k^s\alpha}\alpha + E_{k^s\psi}\psi$ ,  $(N\pi)_\ell = \delta E_{\ell\theta}\theta^k + E_{\ell\psi}\psi$ . Here each  $E_\bullet$  is a matrix with entries in  $\{0, 1\}$  to ensure dimensional consistency of the matrix-vector products. The matrix  $A_\omega$  encodes  $(\omega_{it} - \omega_{jt})$  in the  $g$ -stationarity rows, and  $(A_{\mu y})_{kt} = \sum_{i \in I} \text{PTDF}_{ki} y_{it}$ . All remaining block rows are zero.

The constant vector  $q$  in (41) collects the constant terms in the KKT inequality constraints. Its nonzero blocks are  $q_d = -\vec{b}^0$ ,  $q_g = \vec{C}^0$ ,  $q_\lambda = \vec{G}$ ,  $q_{\mu^1} = \vec{F}$ ,  $q_{\mu^2} = \vec{F}$ ,  $q_p = \text{Cap}$ ,  $q_v = \vec{g}^c$ , and  $q_\ell = (1 - \delta)\vec{e}$ , where each arrow denotes the vector obtained by stacking and replicating the corresponding parameter to match the dimension of the associated block of  $z$ . All remaining blocks of  $q$  are zero.

The vector  $r$  in (41) collects the right-hand sides of the equality constraints whose multipliers are free variables. The only nonzero blocks are  $r_\eta = \vec{g}^c$  and  $r_\psi = \vec{q}_B$ , where  $\vec{q}_B$  stacks  $\{q_b\}$  and is replicated over  $t$ . All remaining components of  $r$  are zero.

## REFERENCES

- [1] N. Jones, "How to stop data centres from gobbling up the world's electricity," *Nature*, vol. 621, pp. 670–673, 2018.
- [2] M. Terrell, "New nuclear clean energy agreement with Kairos Power," [blog.google/outreach-initiatives/sustainability/google-kairos-power-nuclear-energy-agreement/](https://blog.google/outreach-initiatives/sustainability/google-kairos-power-nuclear-energy-agreement/).
- [3] H. Dou, Y. Qi, W. Wei, and H. Song, "Carbon-aware electricity cost minimization for sustainable data centers," *IEEE Transactions on Sustainable Computing*, vol. 2, no. 2, pp. 211–223, 2017.
- [4] T. Dandres, R. Farrahi Moghaddam, K. K. Nguyen, Y. Lemieux, R. Samson, and M. Cheriet, "Consideration of marginal electricity in real-time minimization of distributed data centre emissions," *Journal of Cleaner Production*, vol. 143, pp. 116–124, 2017.
- [5] V. Paramanayakam, A. Karatzas, D. Stamoulis, and I. Anagnostopoulos, "Ecomap: Sustainability-driven optimization of multi-tenant dnn execution on edge servers," *IEEE Transactions on Computers*, vol. 74, no. 11, pp. 3925–3937, 2025.
- [6] I. Gouri, W. Katsak, K. Le, T. D. Nguyen, and R. Bianchini, "Parasol and greenswitch: managing datacenters powered by renewable energy," in *Proceedings of the Eighteenth International Conference on Architectural Support for Programming Languages and Operating Systems*, ser. ASPLOS 13. New York, NY, USA: Association for Computing Machinery, 2013, pp. 51–64.
- [7] Z. Liu, Y. Chen, C. Bash, A. Wierman, D. Gmach, Z. Wang, M. Marwah, and C. Hyser, "Renewable and cooling aware workload management for sustainable data centers," ser. SIGMETRICS '12. New York, NY, USA: Association for Computing Machinery, 2012, p. 175–186.
- [8] S. Naganandhini, C. Sundar, R. Sathya, and G. Venkatesan, "Towards energy-efficient data centres: A comprehensive analysis of cooling strategies for maximizing efficiency and sustainability," in *2023 Intelligent Computing and Control for Engineering and Business Systems (ICCEBS)*, 2023, pp. 1–6.
- [9] J. Dodge, T. Prewitt, R. Tachet des Combes, E. Odmark, R. Schwartz, E. Strubell, A. S. Luccioni, N. A. Smith, N. DeCario, and W. Buchanan,

- “Measuring the carbon intensity of ai in cloud instances,” in *Proceedings of the 2022 ACM Conference on Fairness, Accountability, and Transparency*, ser. FAccT ’22. New York, NY, USA: Association for Computing Machinery, 2022, p. 1877–1894.
- [10] J. Stojkovic, C. Zhang, I. n. Goiri, J. Torrellas, and E. Choukse, “Dynamollm: Designing llm inference clusters for performance and energy efficiency,” in *2025 IEEE International Symposium on High Performance Computer Architecture (HPCA)*, 2025, pp. 1348–1362.
- [11] I. Hasan, Y. Sang, D. Irwin, and G. Zakeri, “Optimal data center load scheduling in power system operation,” in *2025 57th North American Power Symposium (NAPS)*, 2025, pp. 1–6.
- [12] J. Lindberg, B. C. Lesieutre, and L. A. Roald, “Using geographic load shifting to reduce carbon emissions,” *Electric Power Systems Research*, vol. 212, p. 108586, 2022.
- [13] SFGATE, “California has a huge solar power problem. a fix is coming,” <https://shorturl.at/yuRCl>.
- [14] K. Kim, F. Yang, V. M. Zavala, and A. A. Chien, “Data centers as dispatchable loads to harness stranded power,” *IEEE Transactions on Sustainable Energy*, vol. 8, no. 1, pp. 208–218, 2017.
- [15] F. Yang and A. A. Chien, “Large-scale and extreme-scale computing with stranded green power: Opportunities and costs,” *IEEE Transactions on Parallel and Distributed Systems*, vol. 29, no. 5, pp. 1103–1116, 2017.
- [16] A. A. Chien, R. Wolski, and F. Yang, “The zero-carbon cloud: High-value, dispatchable demand for renewable power generators,” *The Electricity Journal*, vol. 28, no. 8, pp. 110–118, 2015.
- [17] Facebook, “Facebook’s U.S. renewable energy impact study,” <https://www.rti.org/publication/facebook-u-renewable-energy-impact-study/fulltext.pdf>, last opened: 2025.
- [18] Microsoft, “Modular Datacenter overview,” <https://learn.microsoft.com/en-us/previous-versions/azure/mdc/mdc-overview>, last opened: 2025.
- [19] Y. Chen, A. L. Liu, and B. F. Hobbs, “Economic and emissions implications of load-based, source-based, and first-seller emissions trading programs under California AB32,” *Operations Research*, vol. 59, no. 3, pp. 696–712, 2011.
- [20] B. Hobbs, “Linear complementarity models of Nash-Cournot competition in bilateral and poolco power markets,” *IEEE Transactions on Power Systems*, vol. 16, no. 2, pp. 194–202, 2001.
- [21] S. A. Gabriel, A. J. Conejo, J. D. Fuller, B. F. Hobbs, and C. Ruiz, *Complementarity Modeling in Energy Markets*, ser. International Series in Operations Research & Management Science. New York, NY: Springer, 2012, vol. 180.
- [22] S. Chen, A. J. Conejo, R. Sioshansi, and Z. Wei, “Equilibria in electricity and natural gas markets with strategic offers and bids,” *IEEE Transactions on Power Systems*, vol. 35, no. 3, pp. 1956–1966, 2020.
- [23] Y. Chen and B. Hobbs, “An oligopolistic power market model with tradable NOx permits,” *IEEE Transactions on Power Systems*, vol. 20, no. 1, pp. 119–129, 2005.
- [24] V. Virasjoki, P. Rocha, A. S. Siddiqui, and A. Salo, “Market impacts of energy storage in a transmission-constrained power system,” *IEEE Transactions on Power Systems*, vol. 31, no. 5, pp. 4108–4117, 2016.
- [25] S. El Khatib and F. D. Galiana, “Negotiating bilateral contracts in electricity markets,” *IEEE Transactions on Power Systems*, vol. 22, no. 2, pp. 553–562, 2007.
- [26] N. Fabra and G. Llobet, “Designing contracts for the energy transition,” *International Journal of Industrial Organization*, vol. 102, p. 103173, 2025, 51st Annual Conference of European Association for Research in Industrial Economics, Amsterdam, 2024.
- [27] F. C. Schweppe, M. C. Caramanis, R. D. Tabors, and R. E. Bohn, *Spot Pricing of Electricity*. Boston, MA: Springer, 1988, reprinted 2013.
- [28] C. Metzler, B. F. Hobbs, and J.-S. Pang, “Nash–Cournot equilibria in power markets on a linearized DC network with arbitrage: Formulations and properties,” *Networks and Spatial Economics*, vol. 3, no. 2, pp. 123–150, 2003.
- [29] R. Goonatillake and R. Bachnak, “Modeling latency in a network distribution,” *Netw. Commun. Technol.*, vol. 1, pp. 1–11, 2012. [Online]. Available: <https://api.semanticscholar.org/CorpusID:27211784>
- [30] G. Wilkins, S. Keshav, and R. Mortier, “Offline energy-optimal llm serving: Workload-based energy models for llm inference on heterogeneous systems,” *SIGENERGY Energy Inform. Rev.*, vol. 4, no. 5, p. 113–119, Apr. 2025.
- [31] M. C. Ferris and T. S. Munson, “Complementarity problems in gams and the path solver1,” *Journal of Economic Dynamics and Control*, vol. 24, no. 2, pp. 165–188, 2000.
- [32] Artelys, “Knitro: The most advanced solver for nonlinear optimization,” <https://www.artelys.com/solvers/knitro/>, last opened: 2025.
- [33] Gurobi, “Gurobi 13.0: Decision intelligence for enterprises,” <https://www.gurobi.com/>, last opened: 2025.
- [34] L. Hirth, T. M. Khanna, and O. Ruhnau, “How aggregate electricity demand responds to hourly wholesale price fluctuations,” *Energy Economics*, vol. 135, p. 107652, 2024.
- [35] A. J. Wood, B. F. Wollenberg, and G. B. Sheblé, *Power generation, operation, and control*. John Wiley & sons, 2013.
- [36] Y. Chen and A. L. Liu, “Emissions trading, point-of-regulation and facility siting choices in the electric markets,” *Journal of Regulatory Economics*, vol. 44, no. 3, pp. 251–286, 2013.
- [37] C. Grigg, P. Wong, P. Albrecht, R. Allan, M. Bhavaraju, R. Billinton, Q. Chen, C. Fong, S. Haddad, S. Kuruganty, W. Li, R. Mukerji, D. Patton, N. Rau, D. Reppen, A. Schneider, M. Shahidehpour, and C. Singh, “The IEEE Reliability Test System-1996. A report prepared by the reliability test system task force of the application of probability methods subcommittee,” *IEEE Transactions on Power Systems*, vol. 14, no. 3, pp. 1010–1020, 1999.
- [38] J. Wang, N. Redondo, and F. Galiana, “Demand-side reserve offers in joint energy/reserve electricity markets,” *IEEE Transactions on Power Systems*, vol. 18, no. 4, pp. 1300–1306, 2003.
- [39] A. Peskoe and E. Martin, “Extracting profits from the public: How utility ratepayers are paying for big tech’s power,” Harvard Electricity Law Initiative, 2025.
- [40] I. M. L. Azevedo, M. G. Morgan, and L. Lave, “Residential and regional electricity consumption in the U.S. and eu: How much will higher prices reduce CO2 emissions?” *The Electricity Journal*, vol. 24, no. 1, pp. 21–29, 2011.